

# Influence of Pipe-Wall Parameters on Non-Intrusive Planar Capacitive Spatial Filter for Solids Flow Measurement

Abbas Ahmed Al-Shalchi

Mohammed Sahib Al-Khesbak

Department of Electronic and  
Communications Engineering

College of Engineering Al-Nahrain University

## Abstract

The paper proposes installing a planar capacitive spatial filter (PCSF) behind thin walls of a dielectric pipe section to operate as a non-invasive sensor for solids flow measurement. The pipe wall shields the electrodes from erosion caused by solid particle flow. A computational model of the flow sensor incorporating the shielding layer is developed. The model's equations are solved using finite difference and relaxation methods and it is then used to examine the effects of the thickness and dielectric constant of the shield on the amplitude and shape of the flow signals. The results show that making the ratio of the shield thickness to the substrate thickness near to the reciprocal of their respective dielectric constants gives a satisfactory combination of enhancement of sensor sensitivity and obtaining flow signals of smoother shape.

**Keywords:** Non-Intrusive Solids Flow Sensors, Capacitive Spatial Filters.

## 1-Introduction

The measurement of solids mass flow rate in pneumatic conveyors is of major importance in many industrial applications and has long been a subject of intensive research in many academic institutions and industrial establishments [ 1, 2 ] . Various technologies have been brought in over the past decades to develop sensors for the flow of particulate materials; the earlier ones utilized mechanical sensors which were obstructive/constrictive [3], while in subsequent systems emphasis shifted to non-obstructive and/or noninvasive methods [4].

The measurement of solids mass flow rate requires knowledge of two parameters: the flow velocity of the solid phase and the concentration of the solids. A variety of signal processing techniques have been proposed to extract the flow velocity from the sensor signals among which are correlation methods [2] and spatial filtering methods [5].

The correlation method is basically a time domain approach wherein the flow velocity is

inferred from the transit time found by cross correlation of two signals obtained from a pair of flow sensors placed along the pipe.

The spatial filtering method is a frequency domain approach that utilizes an array of sensors to yield a flow signal which has a dominant spectral component related to the flow velocity. One of the earliest versions employed a spatial filter called the space-periodic capacitance transducer (SPCT) to sense the flow signal while the power spectral density, estimated from the periodogram via the DFT of the signal, was searched to locate the peak [6,7]. The compactness and ruggedness of the monolithic sensing device and the high speed of obtaining the periodogram by using the fast Fourier transform were the main merits of this approach, whereas its drawbacks were spatial bias of the sensors, and the statistical fluctuation of the raw periodogram which can be ameliorated by averaging several periodograms.

To improve the accuracy of estimating the power spectral density of the SPCT flow signal, alternative signal processing approaches were explored such as the maximum entropy method [8] and searching the wavelet transform (or scalogram) of the flow signal [9]. An implementation of the spatial filtering method using an electrostatic sensor and wavelet-based filters to smooth the power spectrum of the flow signal has also been reported [10]. Other workers attempted to apply neural networks and electrostatic sensors to measure mass flow rate of particulates [1].

In view of the abrasive nature of particulate flow, even non-obstructive sensors are liable to be eroded; this can affect the shape and dimensions of the sensor thereby deteriorating the flow signal and leading to possible inaccuracy in the measurement of flow. Covering the electrode with a dielectric shield should protect it against erosion but its effects on the performance of the flow sensor need to be studied. This work therefore investigates the effects of the thickness and dielectric constant of the shielding layer on the flow signal of the SPCT. Since this work deals only with the sensors without the front end electronics it would be more appropriate to call

this device the planar capacitive spatial filter (PCSF).

### 2 The Planar Capacitive Spatial Filter (PCSF)

The PCSF is a space-periodic planar arrangement of small and closely spaced electrodes, where each alternate electrode is earthed as shown in Fig.(1) which is a longitudinal section view of the PCSF and the surrounding pipe. The electrodes are to be deposited on a ceramic substrate or base layer such as alumina having thickness  $t$  and a dielectric constant  $\epsilon_B$  equal to 10.

The region occupied by an active electrode (A), and half of a grounded electrode (G) on either side will be termed a *cell*. A layer of screening electrodes is placed on the underside of the substrate and is maintained at the same potential as the active sensors to drive the electric

flux lines towards the channel. The shielding layer above the sensor plane is also shown. The upper boundary of the cell represents the upper wall of the flow channel and is considered to be a grounded conductor at zero potential.

The span of the cell  $\lambda$  determines the spatial period of the flow signal. The active electrodes are connected in such a way as to form two interdigital combs separated by a grounded track. In the differential mode of operation the voltage signal from one comb is subtracted from that of the other comb which means that signal waveforms contributed by adjacent cells are in antiphase and, therefore, the effective spatial period doubles to  $2\lambda$ . A solid particle travelling at a velocity  $v$  over the sensor line would produce a flow

signal comprising a number of pulses with a dominant spectral component related to the flow velocity.

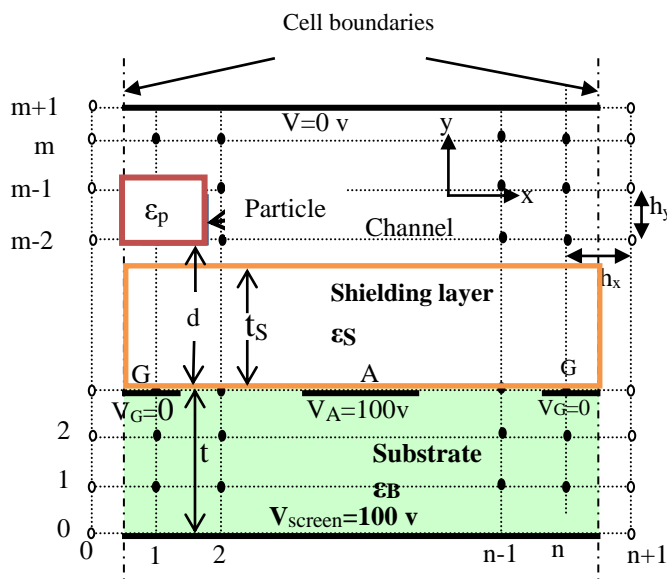


Figure (1) :A single cell of the spatial filter incorporating the shielding layer and covered with a rectangular grid .

### 3 -Mathematical Modelling of the PCSF

The simulation of a PCSF (of infinite depth in the z-direction) responding to a dielectric stimulus travelling in the x-direction is considered here so as to restrict the analysis to a two-dimensional longitudinal section perpendicular to the z-axis. The procedure relies mainly on the computation of the potential field distribution in the cell. In view of the complex boundary conditions in the

SPCT cell this boundary-value problem can not be solved by analytical methods and, hence, a numerical modelling approach based on finite-difference techniques is adopted to solve the model.

The single cell model in Fig.(1) implies that the array of electrodes is of infinite length in the x-direction while a practical spatial filter comprises a finite number of electrodes, as well as being of finite depth in the z direction. Furthermore, numerical models of finite length electrode arrays

were investigated in[11], and the results did not differ significantly from those of the infinite periodic model.

The parameters of the computational model are as follows:  $m=110$ ,  $n=32$ , width of one cell is set to 4mm, cell height is 20mm, substrate thickness ( $t$ ) is 0.901mm ( $5h_y$ ), spacing between adjacent electrode edges is 1mm, length of each sensor is 1mm, particle dimensions are  $1h_x$  by  $1h_y$ , substrate relative permittivity ( $\epsilon_B$ ) is 10, and the relative permittivity of the particle ( $\epsilon_p$ ) is taken to be 100 to simulate a permittivity impulse. The grid pitch sizes  $h_x=0.125$  mm and  $h_y= 0.1802$  mm and all the previously mentioned parameters are fixed throughout all the computational work. The other variable parameters such as particle flying height ( $d$ ) over the sensor line, and shielding layer thickness ( $t_s$ ) are expressed in terms of the substrate or base layer thickness  $t$ . The particle flying height is always measured from the sensor line to the bottom surface of the particle irrespective of whether the sensor is shielded or otherwise.

### 3.1 -Finite Difference Equations for the PCSF Model

For any rectangular grid periodic in the  $x$ -direction with grid-sizes  $h_x$  and  $h_y$ , the coordinates of the  $i$ th,  $j$ th node are given by

$$x_i = ih_x \quad i= 0,1,2, \dots, n+1 \dots \quad (1)$$

and

$$y_j = jh_y \quad j= 0,1,2, \dots, m+1 \dots \quad (2)$$

Nodes corresponding to  $j=0$  and  $j=m+1$  are lower and upper boundary nodes, respectively. The periodicity of the potential field implies that  $V_{0,j} = V_{n,j}$  and  $V_{n+1,j} = V_{1,j}$ .

Most of the nodes lie in regions of homogeneous permittivity; the exceptions being the nodes on the boundaries of the particle, the substrate, and the shielding layer. With reference to Fig.(2), the general form of the finite difference approximation formula which applies at all nodes is given by [12]:

$$V_{i,j} = \frac{2h}{\epsilon_0 W_{i,j}} q_{i,j} + \left[ \frac{\left( W_{i,j}^{(1)} V_{i,j} + W_{i,j}^{(2)} V_{i-1,j} + W_{i,j}^{(3)} V_{i,j+1} + W_{i,j}^{(4)} V_{i,j-1} \right)}{W_{i,j}} \right] \dots \dots \quad (3)$$

$$h = \frac{h_y}{h_x}$$

for  $i = 1, 2, \dots, n$ , and  $j = 1, 2, \dots, m$ ; where  $V_{i,j} = V(ih_x, jh_y)$  is the potential field at the intersection of the  $i$ th column and  $j$ th row in Fig.(1), and

$$\left. \begin{aligned} W_{i,j}^{(1)} &= h^2 (\epsilon_{i,j} + \epsilon_{i,j-1}), \\ W_{i,j}^{(2)} &= h^2 (\epsilon_{i-1,j} + \epsilon_{i-1,j-1}), \\ W_{i,j}^{(3)} &= \epsilon_{i,j} + \epsilon_{i-1,j}, \\ W_{i,j}^{(4)} &= \epsilon_{i,j-1} + \epsilon_{i-1,j-1}, \\ \text{and;} \\ W_{i,j} &= W_{i,j}^{(1)} + W_{i,j}^{(2)} + W_{i,j}^{(3)} + W_{i,j}^{(4)} \end{aligned} \right\} \dots(4)$$

At a node surrounded by a homogeneous dielectric all the  $\epsilon$ 's in eq.(4) have equal values and if there is no free charge,  $q_{i,j} = 0$ , and eq.(3) can be simplified into the form

$$V_{i,j} = \frac{h^2 (V_{i+1,j} + V_{i-1,j}) + V_{i,j+1} + V_{i,j-1}}{2(h^2 + 1)} \dots(5)$$

which is the finite difference approximation to Laplace's equation.

### 3.2-Solving the Model Equations via the SOR Method

The electric potential field in the PCSF region can be computed by using Eqs.(3) to (5) through an iterative approach, such as the well-known successive overrelaxation(SOR) method [12,13].

The SOR formula for finding the potential field everywhere in the SPCT cell is [13 ] :

$$V^{(k+1)}_{i,j} = (1 - \omega) V^{(k)}_{i,j} + \omega \left[ \frac{2h}{\epsilon_o W_{i,j}} q_{i,j} + \frac{W^{(1)}_{i,j} V^{(k)}_{i+1,j} + W^{(2)}_{i,j} V^{(k+1)}_{i-1,j} + W^{(3)}_{i,j} V^{(k)}_{i,j+1} + W^{(4)}_{i,j} V^{(k+1)}_{i,j-1}}{W_{i,j}} \right]$$

for  $i = 1, \dots, n, j = 1, \dots, m.$  ..... (6)

where  $\omega$  is the relaxation factor ( $1 < \omega < 2$ ) and  $k$  is the iteration number. In this work it was found, by investigating the effect of  $\omega$  on the time taken to reach the solution, that a good empirical choice of  $\omega$  is 1.8.

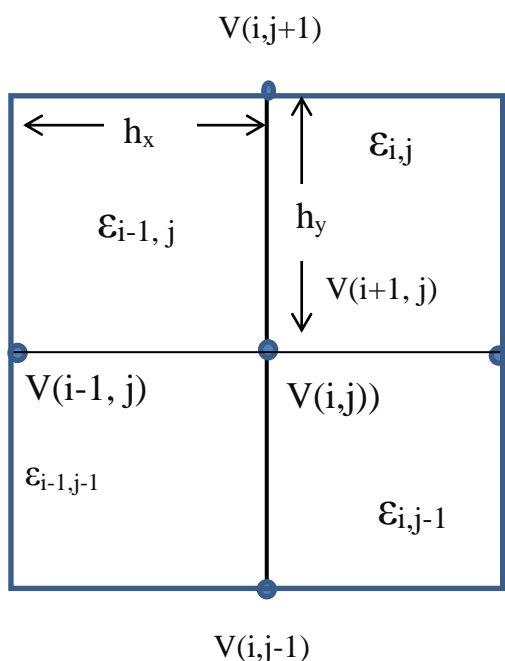


**Figure (2):**A mesh point in a multi-dielectric region

#### 4-Effective and Incremental Capacitance Waveforms for the Unshielded Sensor

Before dealing with the flow signals of the shielded sensors, the ones from the unshielded sensor need to be found so that comparisons can be made. These are basically capacitance signals which are converted into voltage signals by the signal conditioning circuits.

The effective capacitance  $C_{eff}$  is the total equivalent capacitance seen between the active

electrode (sensor) and the ground of the system. It is defined as

$$C_{eff} = Q_{eff} / V_A \dots \dots \dots (7)$$

where  $V_A$  is the active electrode voltage (arbitrarily set at 100V for convenience) and  $Q_{eff}$  is the total charge on the electrode, which is the sum of the active electrode node charges. Each node charge can be found by solving for  $q_{i,j}$  in eq (3) after the potential distribution for the unknown  $V_{i,j}$ 's around the electrode line has converged.

The effective capacitance waveforms for an unshielded sensor responding to a particle moving with constant velocity inside one cell of the PCSF for different particle flying heights ( $d$ ) were obtained using eq.(7) and eq.(3). Each trace of the effective capacitance signal has a non-zero average value which is eliminated by the signal conditioning stage after converting the signal into a voltage. For simplicity the output signal will be represented as a capacitance signal called the incremental capacitance signal which has dimensions of farads per meter of depth in the  $z$  direction. These incremental capacitance waveforms are presented in Fig.(3) for different values of  $d$  for a span of two cells (8 mm) to illustrate differential mode operation.

It was found that the signal waveforms for the case of a particle passing close to the **unshielded** sensors at altitudes of  $d=0$  and  $d=0.2t$  have spikes or sharp points as shown in Figs.(4a) and(4b)respectively; these are undesirable owing to their high harmonic content. Also some of these signals ( from particles close to the sensors plane) suffer from the presence of half cycle secondary lobes and half cycle cavity or dip problems which were shown before in Fig.(3) and are also undesirable.

#### 5 Potential Field and Electric Charge Distribution on the Shielded Sensor Electrode in an Empty Channel

The finite difference model equations were solved to find the potential distribution for the

shielded sensor. This is shown in Fig.(5) for part of the PCSF cell. The ridge at  $j=5$  beneath which the active electrode lies can be clearly seen and a second ridge appears at  $j=8$  which gives the potential along the boundary between the shielding layer (which has a thickness of  $3h_y$  and  $\epsilon_s=4$ ) and the flow channel.

The charge distribution along the active electrode was also computed using eq.(3) and is shown in Fig.(6). The sensor electrode spans eight nodes. and the graphs show high concentrations of charge at nodes 1 and 8, i.e., at the edges of the

active electrode. The graphs also show that using a thicker dielectric layer leads to higher buildup of charge on the electrode which in turn implies higher values of effective capacitance. It must be pointed out, however, that only part of this capacitance namely the capacitance associated with the flux that crosses into the flow channel contributes to the flow signal and hence the incremental capacitance waveforms need to be computed.

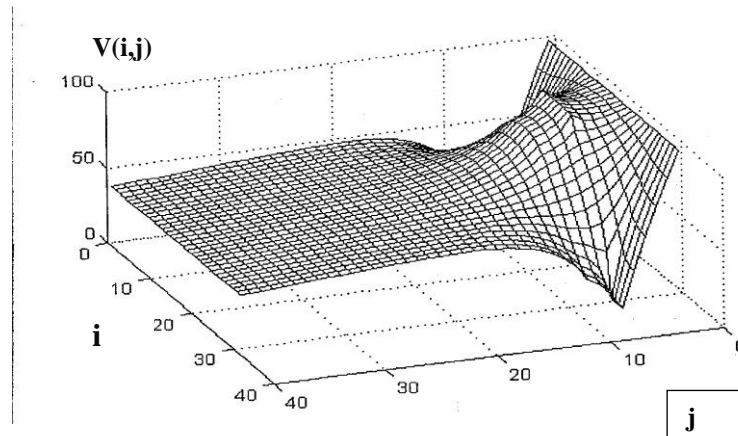


**Figure (5):** Potential distribution in part of a cell of the shielded PCSF (40 rows by 32 columns).

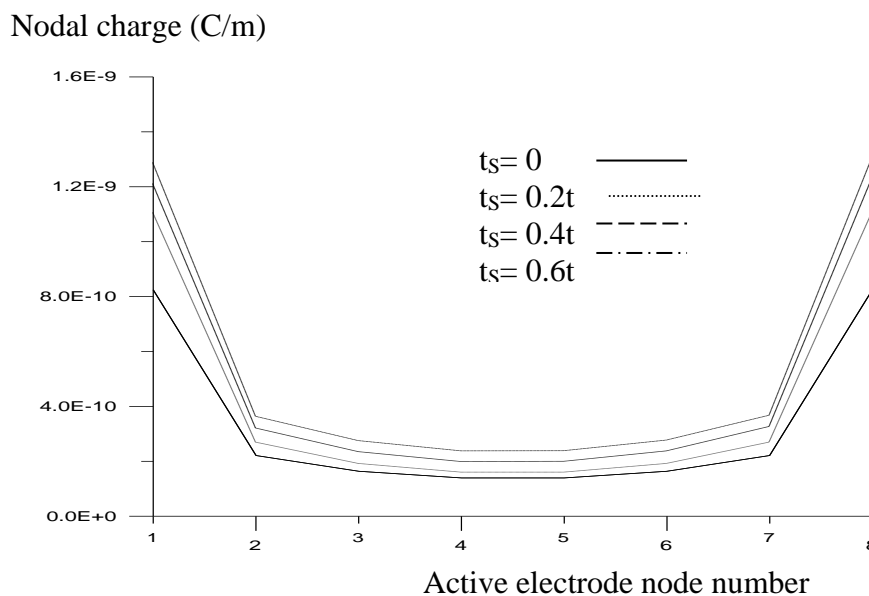


**Figure (6) :** Charge distribution along the active sensor electrode for shielding layer having  $\epsilon_s=4$  and several values of shield thickness.

**6 Effect of the Shielding Layer on the Amplitude of the Flow Signal**

The computational model in Fig.(1) was used to investigate the effect of the thickness of the pipe wall and its dielectric constant on the flow

signal. Particle flying heights were still measured with respect to the sensor line which means that the clearance of the particle over the shielding layer is  $d - t_s$  with  $d \geq t_s$ .

Two graphs in Fig.7(a) show the variation of the (peak-to-peak) amplitude of the incremental capacitance waveforms with the normalized shielding layer thickness ( $t_s/t$ ). The graphs, which are for

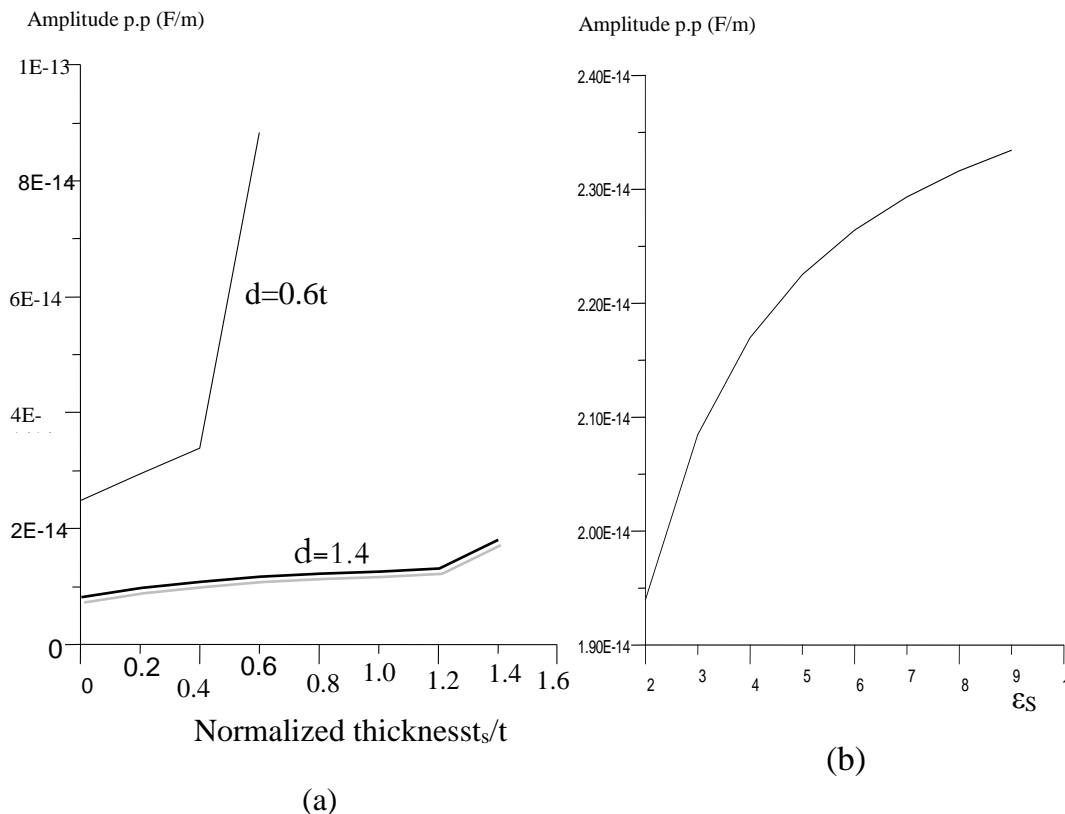


**Figure (7)** Incremental capacitance signal amplitude (peak to peak) versus:

- (a) normalized shielding layer thickness with  $\epsilon_s = 4$ .
- (b) shielding layer permittivity  $\epsilon_s$  with  $d = 1.4t$  and  $t_s = 0.4t$ .

particle altitudes of  $0.6t$  and  $1.4t$  respectively, terminate at the abscissa point  $t_s/t = d/t$  where the particle clearance becomes zero. It can be seen that the presence of a shield layer above the sensors plane causes the signal amplitude to increase thereby improving the sensor sensitivity. The percentage improvement for the lower altitude is more noticeable than that for the higher altitude.

The use of a pipe wall having higher permittivity also enhances the output signal as shown in Fig.7(b). This effect is stronger at lower values of  $\epsilon_s$  and the slope levels off as  $\epsilon_s$  approaches  $\epsilon_B$ .

### 7 Effect of the Shielding Layer on the Distortion in the Flow Signal

A number of incremental capacitance signals for shielding layer thickness of  $2t$  and different values of particle height are displayed in Fig.(8) showing that shielding the PCSF with such a layer will ensure smooth output signals for any particle height within the channel.

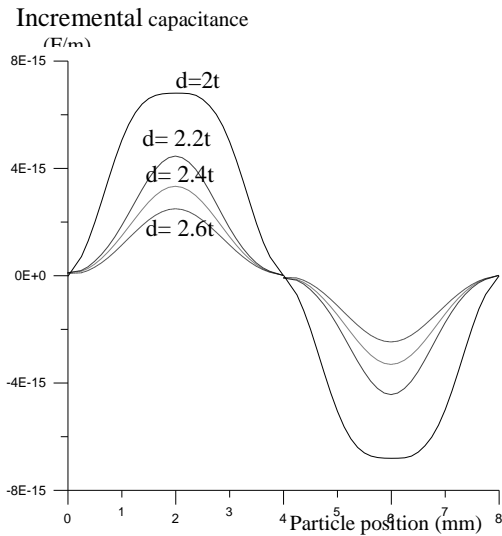


**Figure (8):** Incremental capacitance signals with  $t_s = 2t$  and particle trajectories of  $2t$  and higher

The same pattern of gradual improvement in signal shape with increased shield thickness emerged from extensive inspections of other sets of waveforms for many combinations of shielding layer thicknesses and particle flying heights. The secondary lobes as well as the cavity are removed from all signals for shielding layer thickness  $t_s$  higher than  $2t$ . This gives the limit at which the cavity begins to vanish, as the signal measured when the particle is moving at this level ( $d=t_s=2t$ ) has a flat peak.

Signals for flying heights above  $d=2t$  were found to have smooth nearly-sinusoidal shape for different values of  $t_s$ . However, signals from distant flying heights which had smooth shape prior to shielding were not much influenced by the presence of the shielding layer.

A number of signals are displayed in Figs.(9) and (10) for a particle travelling in a horizontal path touching the surface of the shielding layer ( i.e.,  $d= t_s$ ) for several values of shield thickness. This is the situation which normally gives the highest distortion in flow signal shapes. The waveform produced by the particle moving at  $d= 1.4t$  is common to both figures to facilitate comparisons considering that the two figures have different vertical scales .It can be seen that the cavity in the flow signal disappears when the shielding layer thickness is more than  $2t$ , i.e., more than twice the thickness of the substrate, say  $2.4t$ . This is because the shielding prevents the particle from passing at low flying heights which are too close to the sensors plane. It is interesting to note that this optimal thickness ratio ( $t_s/t = 2.4$

) is approximately equal to the reciprocal of the permittivity ratio ( $\epsilon_s/\epsilon_B$ ).

If the waveforms in Fig.(9) and Fig.(10) which are for the lowest possible particle trajectories above a shielded sensor are compared with their counterparts for the unshielded sensor in Fig.(4), the improvement in signal shape is quite evident.

### 8 Conclusion

In industrial solids flow measurement systems the use of the pipe wall as a shield to protect the sensors in the PCSF from abrasion also makes the PCSF more versatile because it can operate as a non-invasive flow sensor. Additional beneficial effects on the performance of the PCSF are gained such as the enhancement of flow signal amplitude

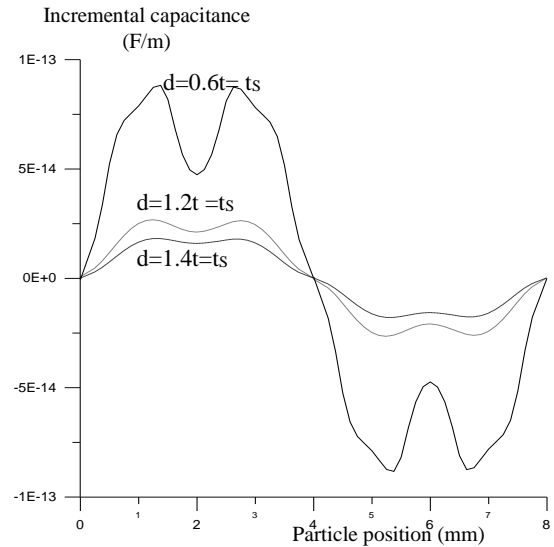


**Figure (9):** Incremental capacitance signals for a particle moving in touch with the surface of the shielding layer of thickness  $t_s=0.6t, 1.2t,$  and  $1.4t$ .

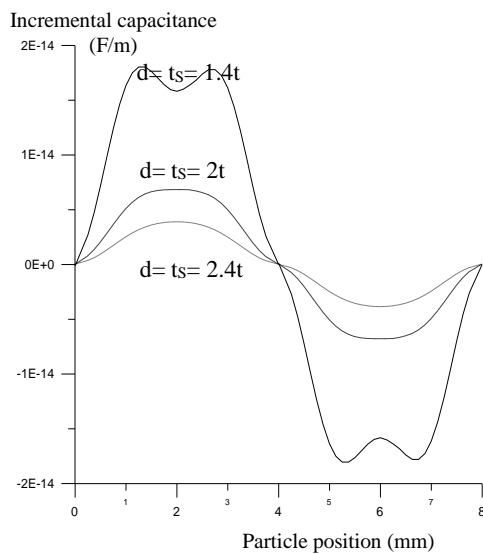


**Figure (10):**Incremental capacitance signals for a particle moving along the surface of the shielding layer having thickness  $t_s = 1.4t$ ,  $2t$ , and

when the thickness of the shield is increased up to a certain limiting value proportional to the substrate thickness, and to the ratio of the dielectric constant of the substrate to that of the shield.

Flow signal shape is also improved as the shielding layer interposes between the sensors and the flowing particles, preventing them from passing through regions that distort the signal shape.

### 9. References

[1] Y. Yan, L. Xu, P. Lee, "Flow Measurement of Fine Particles in a Pneumatic Suspension Using Electrostatic Sensing and Neural Network Techniques," *IEEE Trans. on Instrumentation and Measurement*, Vol.55, No.6, p.2330 – 2334, Dec. 2006.

[2] A. Fuchs, H. Zangl, G. Brasseur, E.M. Petriu, "Flow Velocity Measurement for Bulk Granular Solids in Pneumatic Conveyor Pipes Using Random Correlator Architecture," *IEEE Trans. on Instrumentation and Measurement*, Vol.55, No.4, p.1228 – 1234, Aug. 2006.

[3] M.S. Beck, N. Wainwright, "Current Industrial Methods of Solids Flow Detection and Measurement," *Powder Technology*, Vol.2, p.189-197, 1968/1969.

[4] Y. Yan, "Mass Flow Measurement of Bulk Solids in Pneumatic Pipelines," *Measurement Science and Technology*, Vol.7, No.12, p.1687-1706, 1996.

[5] D. Hrach, A. Fuchs, H. Zangl, "Capacitive Flowmeter for Gas-Solids Flow Applications

Exploiting Spatial Frequency," *IEEE Sensors Applications Symposium*, Atlanta, Ga., 12-14 Feb. 2008.

[6] E.M. Deeley and A. Al-Shalchi, "Space Periodic Capacitance Transducer for the Measurement of Flow Velocity," *IEE Proc.-D (GB)*, Vol. 129, No. 4, pp. 105-112, July 1982.

[7] A. A Al-Shalchi, 'Space Periodic Capacitance Transducers for Measurement of Particulate Flows,' Ph.D. Thesis, University of London, 1981.

[8] A. A. Al-Shalchi, R.G. Hermiz, "Solids Flow Velocity Measurement by the Maximum Entropy Method," *Journal of Nahrain University – Engineering*, Vol.1, No.1, p.45 – 68, Dec.1996.

[9] M.K.A. Al-Saadi, "Decomposition of the Space-Periodic Capacitance Transducer Signals Using the Wavelet Transform," M.Sc. Thesis, Nahrain University, Baghdad, Iraq, Oct.1999.

[10] C.L. Xu, G. Tang, B. Zhou, S. Wang, "The Spatial Filtering Method for Solid Particle Velocity Measurement Based on an Electrostatic Sensor," *Measurement Science and Technology*, Vol.20, No.4, 2009.

[11] N.I. Abbas, "Modeling of Finite Length Space-Periodic Capacitance Transducer Using Finite-Difference Methods," M.Sc. Thesis, University of Technology, Baghdad, Iraq, Sept. 1990.

[12] M.B. Allen III, I. Herrera, and G.F Pinder, "Numerical Modeling in Science and Engineering," John Wiley and Sons, New York, 1988.

[13] L. A. Hageman and D.M Young, "Applied Iterative Methods," Academic Press Inc., New York, 1981.

[14] A. A. Al-Shalchi and L.A. Salman, "Computer Modeling of the Response of a Space Periodic Capacitance Transducer Using a Combined SOR-FFT Method," *Proceedings of the Second Scientific Conference on Computers and Their Applications (SCCA'98)*, p.171-176, Applied Science University, Amman, Jordan, 21-28 September 1998.

## تأثير متغيرات جدار الأنبوب على مرشح مكاني لاتداخلي سعوي مسطح لأغراض قياس تدفق الجسيمات

محمد صاحب محمدعلي الخسباك  
كلية الهندسة - جامعة النهريين

عباس أحمد الشالحي  
كلية الهندسة-جامعة النهريين

### الخلاصة:

يعرض هذا البحث مقترح وضع مرشح مكاني سعوي مسطحسمي المديلة السعوية المتواترة مكانيا خلف جدار رقيق لمقطع عازل من أنبوب التدفق ليعمل متحسسا لاتداخليا لقياس تدفق الجسيمات. الجدار بقي الأقطاب الكهربائية من التآكل الذي يسببه تدفق الجسيمات الصلدة. وقد جرى تطوير نموذج حاسوبي للمديلة السعوية يحتوي على الطبقة الحاجبة وحُلَّت معادلات النموذج باستخدام طريقة الفروقات المتناهية والتراخي المفرط المتتابع لأستحصال مجال الجهد الكهربائي ومن ثم استخدم لدراسة تأثير سماكة الطبقة الحاجبة وثابت عزلها الكهربائي علناتساع و شكل اشارات التدفق النتائج المستحصلة تبين إن جعل نسبة سماكة الطبقة الحاجبة الى سماكة الطبقة الواقية مقارنة لمقلوب نسبة ثابتي عزلهما تجمع بشكل مقبول بين تقوية حساسية المجس والحصول على اشارات تدفق اكثر ملاسة.